Am J Cancer Res 2023;13(6):2617-2629
www.ajcr.us /ISSN:2156-6976/ajcr0149737

Original Article

Cuproptosis-related LINC01711 promotes the progression of kidney renal clear cell carcinoma

Houliang Zhang[1*], Yifan Zhang[2*], Liu Gao[3*], Wei Song[2], Haipeng Zhang[2], Guangcan Yang[2], Yidi Wang[2], Jinliang Ni[2], Keyi Wang[2], Guangchun Wang[2], Weipu Mao[1,4]

[1]Department of Urology, Shanghai Putuo District People's Hospital, School of Medicine, Tongji University, Shanghai 200060, China; [2]Department of Urology, Shanghai Tenth People's Hospital, School of Medicine, Tongji University, Shanghai 200072, China; [3]Bengbu Medical College, Bengbu 233000, Anhui, China; [4]Department of Urology, Affiliated Zhongda Hospital of Southeast University, Nanjing 210009, Jiangsu, China. [*]Equal contributors.

Received February 18, 2023; Accepted May 25, 2023; Epub June 15, 2023; Published June 30, 2023

Abstract: This study utilized The Cancer Genome Atlas (TCGA) database to identify cuproptosis-related long non-coding RNAs (CRlncRNAs) in patients with kidney renal clear cell carcinoma (KIRC) which was further applied to construct risk signatures. All KIRC patients were divided into the training and the validation sets at a ratio of 7:3. Lasso regression analysis identified two prognosis-associated CRlncRNAs (LINC01204 and LINC01711), and prognostic risk signatures were constructed in both the training and the validation sets. Kaplan-Meier survival curves showed that patients with high-risk scores had significantly shorter overall survival (OS) than those with low-risk scores both in both the training and the validation sets. The area under the curve (AUC) of the prognostic nomogram generated based on age, grade, stage and risk signature to predict the 1-, 3- and 5-year OS were 0.84, 0.81 and 0.77, respectively, and the calibration curves also showed the high accuracy of the nomogram. In addition, we constructed the LINC01204/LINC01711-miRNA-mRNA ceRNA network graph. Finally, we experimentally investigated the function of LINC01711 by knocking down LINC01711 and revealed that knockdown of LINC01711 inhibited the proliferation, migration and invasion of KIRC cells. Hence, in this study, we developed a signature of prognostic risk-associated CRlncRNAs that could accurately predict the prognosis of KIRC patients and constructed a related ceRNA network to shed light on the mechanistic study of KIRC. LINC01711 might serve as a potential biomarker for the early diagnosis and prognosis of KIRC patients.

Keywords: Cuproptosis, kidney renal clear cell carcinoma, LncRNAs, LINC01204, LINC01711

Introduction

As one of the most prevalent malignancies of the urinary system, the incidence and mortality of renal cell carcinoma (RCC) are increasing globally in recent decades. There were over 430,000 new RCC diagnoses and 179,000 deaths occurred worldwide in 2020 [1]. The most common histological subtype of RCC is kidney renal clear cell carcinoma (KIRC), which accounts for approximately 75-80% of all kidney cancer cases [2]. The development of KIRC is associated with multiple genetic mutations and protein interactions. For example, the mutation, hypermethylation, deletions and biallelic inactivation of the von Hipple-Lindau (VHL) gene, a tumor suppressor gene on chromosome 3 that regulates the cellular response to hypoxia through hypoxia-inducible factor-1 (HIF-1) [3], have been found to be strongly associated with most KIRC [4]. Therefore, elucidating the molecular mechanisms underlying KIRC tumorigenesis is important for the development of clinical therapies.

Copper is an essential trace metal, and its level is critical for normal physiological functions, as abnormal copper level can either weaken the function of metal-binding enzymes or lead to cell death [5]. Several studies have demonstrated that the copper level is upregulated in various malignancies compared to normal tissues, such as breast cancer [6], thyroid cancer [7], lung cancer [8], prostate cancer [9], and gallbladder cancer [10]. Furthermore, copper has been proven to play a prominent role in the eti-

ology and the progression of tumors [11]. Specifically, copper can promote angiogenesis by activating several angiogenic factors, including vascular endothelial growth factor (VEGF), angiogenin (hAng), fibroblast growth factor 1 (FGF1) and interleukin 1 (IL-1). Notably, cupper can stabilize nuclear hypoxia-inducible factor-1 (HIF-1), which further increases the expression of angiogenic factors [12, 13]. Recently, Tsvetkov et al. [14] found that the intracellular copper accumulation could lead to a novel type of programmed cell death (PCD), named cuproptosis. Thus, due to its essential role in cancer progression, copper-related molecules may serve as potential therapeutic targets for KIRC.

Long non-coding RNAs (lncRNAs) are a class of RNA molecules with transcriptional lengths greater than 200 nt in length that are localized in the nucleus or cytoplasm of cells [15]. Initially, lncRNAs were initially thought to be merely non-coding RNAs [16]; however, with the development of new technologies, lncRNAs have been shown to be involved in various biological behaviors of malignancies, including proliferation, differentiation, apoptosis and metastasis [17]. Nevertheless, whether and how cuproptosis-related lncRNAs (CRlncRNAs) influence the progression of KIRC still remain to be determined. Therefore, this study was designed to examine the relationship between cuproptosis and KIRC as well as to identify prognosis related CRlncRNAs and determine their functions in KIRC. By screening CRlncRNAs in patients with KIRC, we identified two CRlncRNAs (LINC01204 and LINC01711) that were associated with prognosis. Moreover, we constructed the LINC01204/LINC01711-miRNA-mRNA ceRNA network graph. Finally, we experimentally explored the function of LINC01711 and revealed that knockdown of LINC01711 inhibited the proliferation, migration and invasion of KIRC cells.

Materials and methods

Data source and data processing

KIRC transcriptome count data were downloaded from the TCGA database and annotated using Homo_sapiens.GRCh38.100.chr.gtf. Data of 495 KIRC patients and 72 normal controls were used and transformed into Transcripts Per Kilobase Million (TPM) data. The lncRNAs and the CRlncRNAs were selected for pearson correlation analysis (abs(cor) > 0.4 and *P* value < 0.05). Using the "limma" package, differentially expressed lncRNAs between patients and normal controls were screened according to the screening criteria of abs(logFC) > 1 and *P* value < 0.05. The intersection set of 46 CRlncRNAs was identified. Since the data were extracted from the TCGA database, ethics committee approval for this study was not required.

Construction of a prognostic risk related CRlncRNAs signature

To construct a prognostic risk model, the clinicopathological data of KIRC were downloaded from the TCGA database. Duplicate samples and data with less than 30 days of follow-up were removed, and thus, a total of 450 clinical samples with complete survival information were included in this study.

These 450 samples were randomly divided into training (315 samples) and validation set (135 samples) at a ratio of 7:3. By using lncRNA expression data combined with survival data, CRlncRNAs associated with prognostic risk were finally selected. The risk score for each sample was calculated by the formula: Risk score = ∑iCoefficient (lncRNAi) * Expression.

Next, we divided these samples into high- and low-risk groups based on their risk scores. The Kaplan-Meier survival curve was applied to compare the overall survival (OS) of patients in the high- and the low-risk groups. Univariate and multivariate Cox proportional risk analyses were conducted by the "rms" package and "survivor" package utilizing the constructed model and the clinical information.

Construction of a nomogram and its validation

A prognostic nomogram for OS was constructed based on the results of multivariate Cox regression analysis, including the risk model, age, stage, and grade. Receiver operating characteristic (ROC) curves and calibration curves were used to assess the predictive value of the nomogram.

Impact of the risk related CRlncRNAs on OS

To further explore the role of the risk related CRlncRNAs in renal clear cell carcinoma, we

first verified the relationship between the risk related CRlncRNAs and clinical variables including T-stage, N-stage, M-stage, tumor stage, and tumor grade. Subsequently, the effect of the risk related CRlncRNAs on the 1-, 3-, and 5-year OS of patients was assessed by constructing Kaplan-Meier survival curves using survminer and survivor package.

Construction of a LncRNA-miRNA-mRNA co-expression network

The risk related CRlncRNAs-binding microRNAs and the microRNAs that bind to cuproptosis-related genes were predicted in TargetScan. MicroRNAs with context++. score. percentile greater than 90 were selected. At the end, nine microRNAs that bound to both LncRNA and cuproptosis-related mRNA were identify.

Patient tissue samples

The tumor samples and the paired normal tissues were obtained from patients who underwent partial or radical nephrectomy in the Department of Urology, Shanghai Tenth People's Hospital, Tongji University. This study was approved by the ethics committee of Shanghai Tenth People's Hospital (SHSY-IEC-4.1/19-211/01). All patients provided written informed consent.

Cell culture and transfection

Human renal cancer cell line 786-O was purchased from the Cell Bank of the Chinese Academy of Sciences (Shanghai, China). Small interference (si) RNAs targeting LINC01711 (si-LINC01711-1: GGUGUCACUAGACAUCCUA; UAGGAUGUCUAGUGACACC. si-LINC01711-2: ACCUUUGUGAGUGUGAUGA; UGGAAACACUCACACUACU) and the scramble siRNA negative control were purchased from Tsingke Biotechnology (Beijing, China). JetPRIME was used as the siRNA transfection agent according to the manufacturer's protocol (YEASEN, China).

RNA extraction and quantitative real-time PCR (RT-qPCR)

Total RNA was extracted from cells by Trizol reagent (Invitrogen, USA). After quantification, 1 μg of RNA was used to synthesize cDNA, which was used as the template in RT-qPCR to determine the relative expression of LINC01711. GAPDH was used as the internal reference.

Fluorescence in situ hybridization (FISH)

Fluorescent probes for the detection of LINC01711 were synthesized by Genepharma (Genepharma Biotechnology, Shanghai, China). Briefly, tissues were fixed with 4% paraformaldehyde and treated with proteinase K. Following pre-hybridization at 37°C for 30 minutes, tissues were hybridized with the LINC01711 probe at 37°C overnight.

Colony formation assay, EdU assay, wound healing assay, and transwell assay

Briefly, colony formation assay was performed as follows: cells at a density of 5^10^2 were plated in the well of 6-well plates and stained with crystal violet solution after 2 weeks of culture. The EdU assay, wound healing assay, and transwell assay were used to assess the proliferation, migration, and invasion of cells, respectively, which were described previously [18].

Statistical analysis

Univariate and multivariate Cox regression models were used for survival analyses. The software used in this study was R-Studio (Boston, USA) and GraphPad Prism 8.3 (San Diego, USA). Continuous variables were presented as mean ± SD. Comparison between two groups was carried out by student t-test, while comparison among multiple groups was conducted by one way analysis of variance (ANOVA). *P* values less than 0.05 were considered statistically significant.

Results

Construction and validation of prognostic signature associated with CRlncRNAs

We first utilized data from TCGA database to screen for differentially expressed lncRNAs and CRlncRNAs in patients with KIRC, and in the intersection between the 1055 differentially expressed lncRNAs and 696 CRlncRNAs, we obtained 46 overlapping lncRNA (**Figure 1A**). Then, two prognostic risk-related CRlncRNAs (LINC01204 and LINC01711) were further identified by using lasso Cox regression (**Figure 1B**, **1C**) and were used to build a risk model. As expected, the high-risk group had significantly

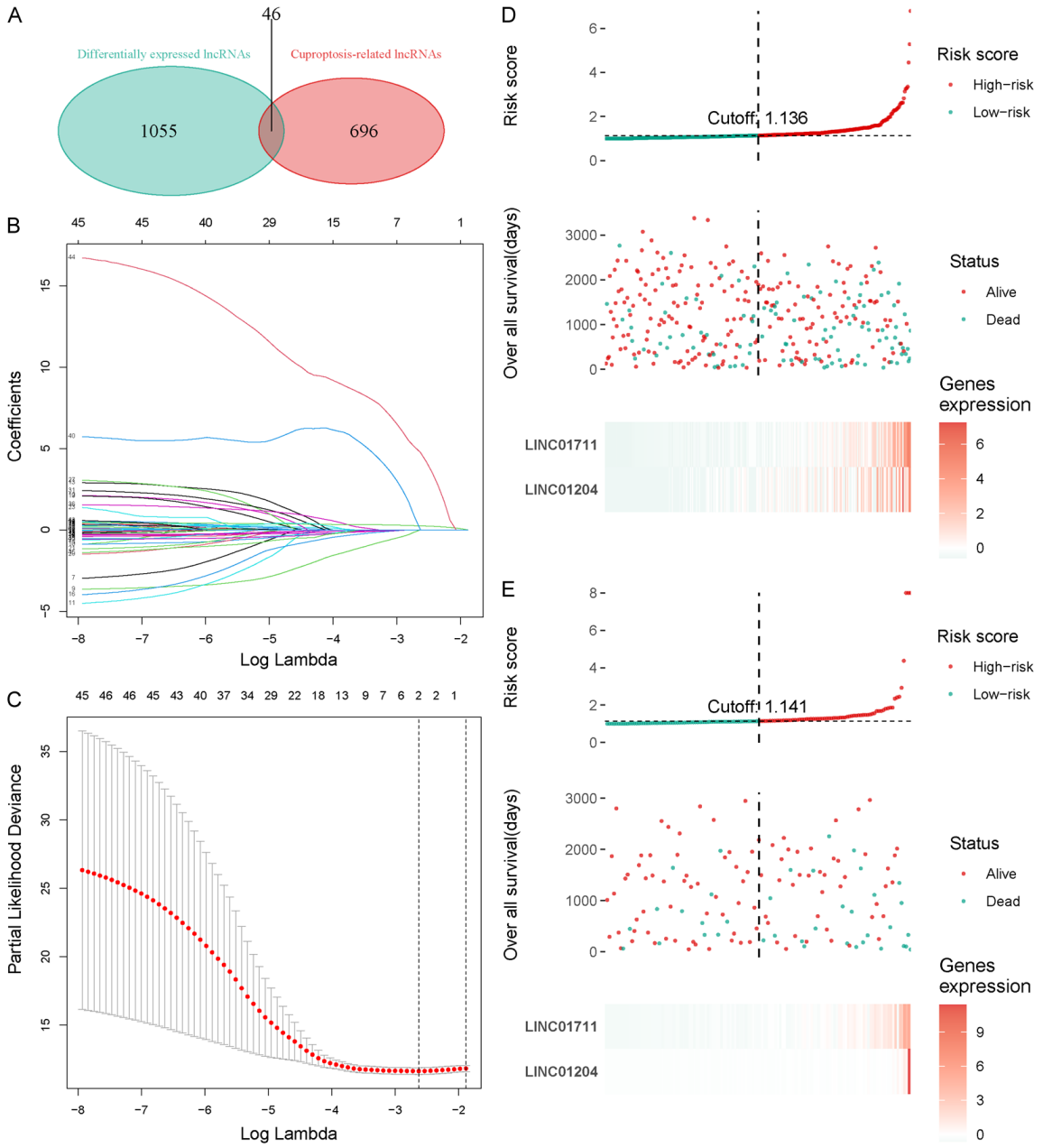

Figure 1. Development of a risk signature consisting of 2 CRlncRNAs to predict KIRC prognosis. (A) Venn Diagrams showing the overlap of lncRNA between differentially expressed lncRNAs and cuproptosis-related lncRNAs. (B) Lasso coefficient profiles of the prognostic CRlncRNAs. (C) Lasso coefficient values and vertical dashed lines at the best log (lambda) value were displayed. (D, E) The risk Score distribution in high- and low-risk score KIRC patients in training group (D) and test group (E).

fewer survival patients than the low-risk group did, as shown by the scatter dot plot in both the training and validation sets. In addition, the heatmap indicated that the high-risk group expressed higher levels of LINC01204 and LINC01711 (**Figure 1D**, **1E**). Together, these results suggested that LINC01204 and LINC01711 were upregulated in high-risk group and were risk factors for the poor diagnosis of KIRC.

Furthermore, the Kaplan-Meier survival curve was applied to compare the survival between the high- and the low-risk group, and the results

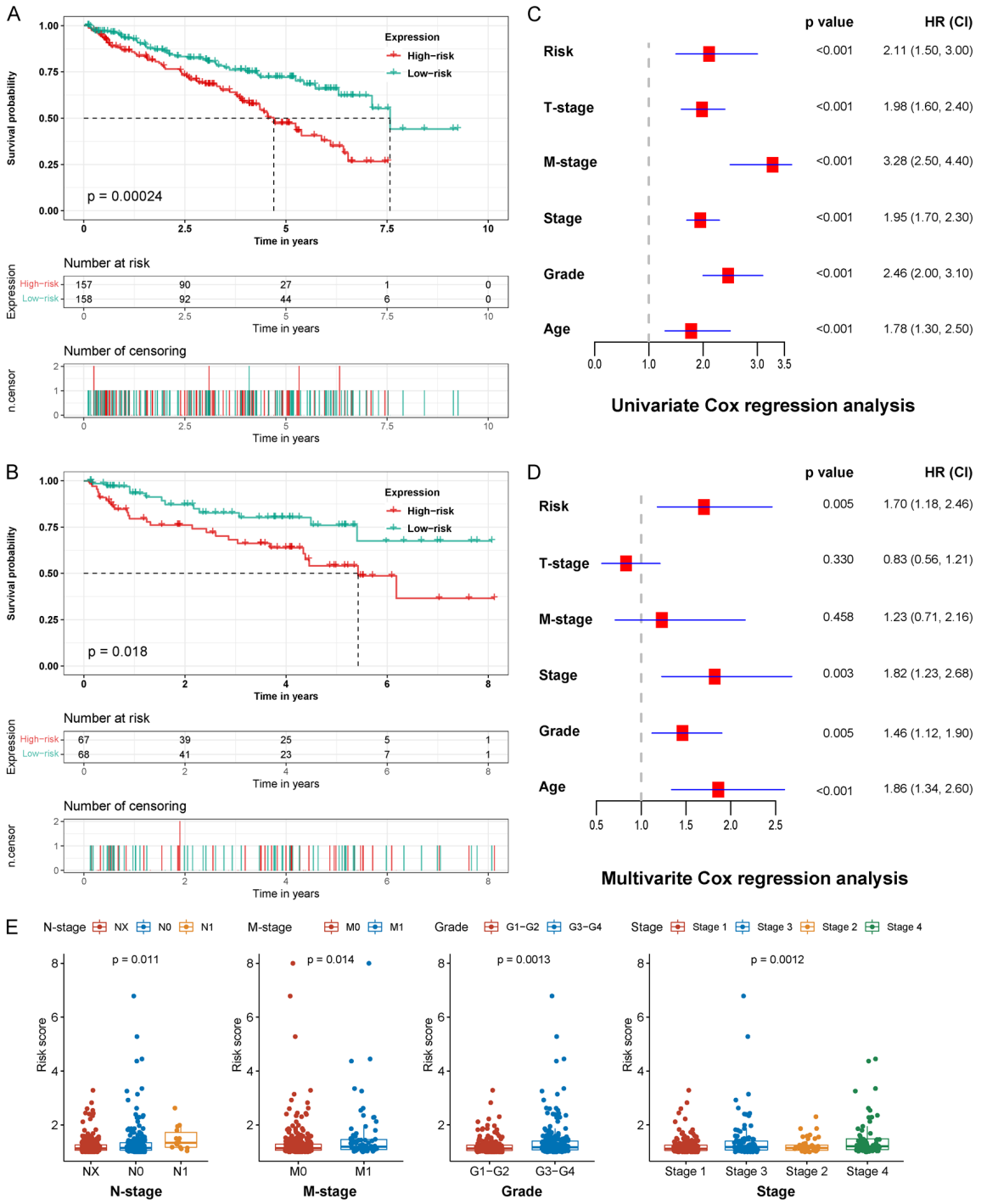

Figure 2. Validation of the accuracy of risk score model. (A, B) Kaplan-Meier survival curve for KIRC patients with high- and low-risk scores in the training group (A) and test group (B). (C) The forest plots for univariate Cox regression analysis showed that risk model, T-stage, M-stage, stage, grade and age were prognostic risk-related variables. (D) The forest plots for multivariate Cox regression analysis showed that risk model, M-stage, stage, grade, and age were prognostic risk-related variables. (E) The relationship between risk model and N stage, M stage, stage and grade.

demonstrated that the high-risk group had significantly shorter OS compared to the low-risk group (training set: P < 0.001; validation set: P=0.018) (**Figure 2A**, **2B**). Moreover, we conducted univariate (**Figure 2C**) and multivariate Cox regression analyses (**Figure 2D**) and found

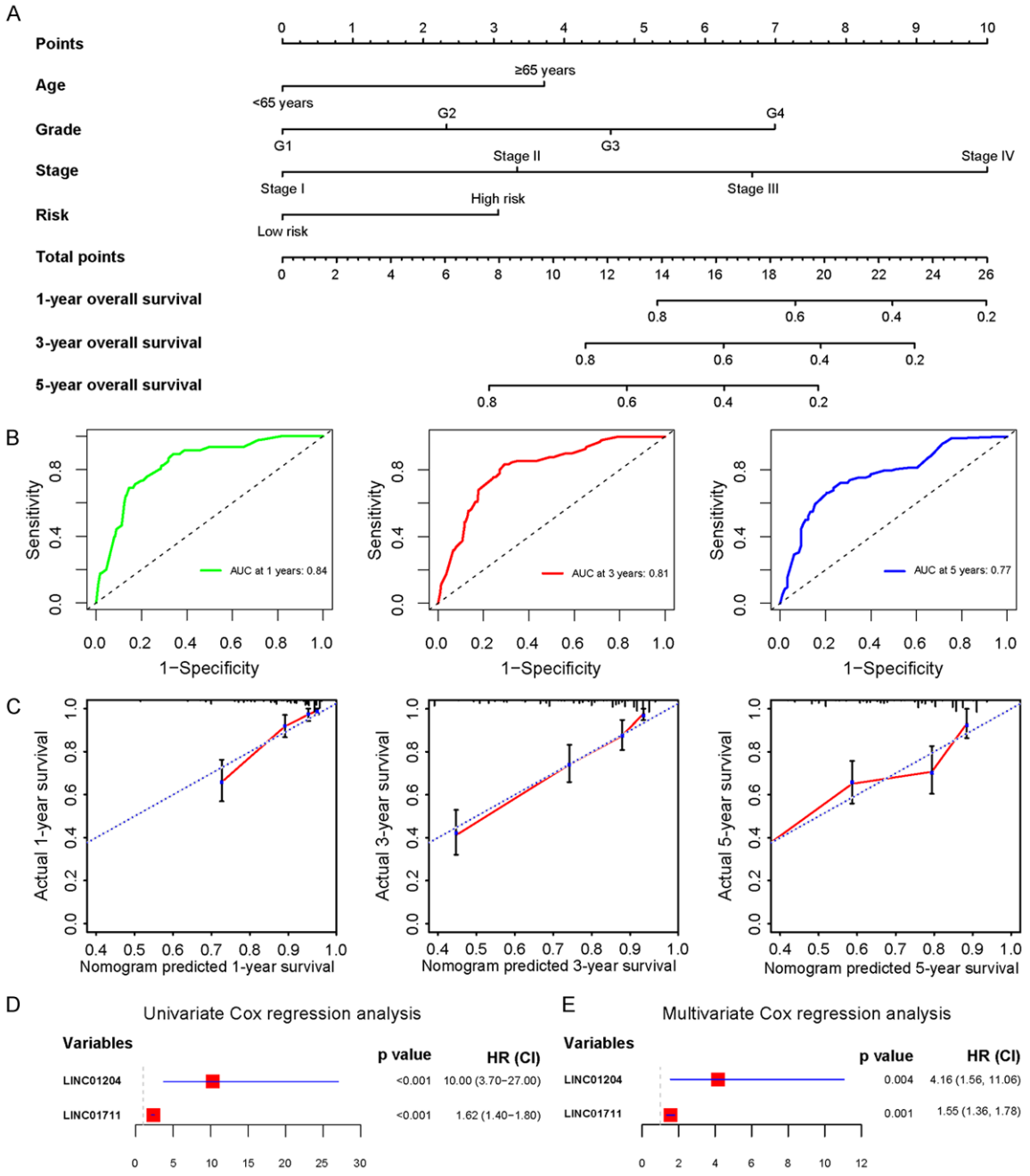

Figure 3. Establishment of a nomogram based on clinicopathological characters including risk model. (A) Prognostic nomograms for KIRC patients were constructed based on risk models and other prognosis-related clinicopathological variables. (B) ROC curves showed that prognostic nomograms were better able to predict 1-, 3-, and 5-year overall survival in KIRC patients. (C) Calibration curves for nomograms showed agreement between predicted and actual survival. (D, E) Univariate (D) and multivariate (E) Cox regression analysis of overall survival related KIRC patients CRlncRNAs.

that pathological stage, risk model, grade, and age were independent prognostic risk factors. Finally, we assessed the relationship of the risk model with N stage, M stage, pathological stage and grade and observed a correlation of high risk score with high tumor grade as well as tumor stage ($P < 0.05$, **Figure 2E**), indicating that the risk model was effective in predicting the prognosis of KIRC.

Establishment of prognostic nomogram

We used four independent prognostic risk factors to construct a nomogram to predict the 1-,

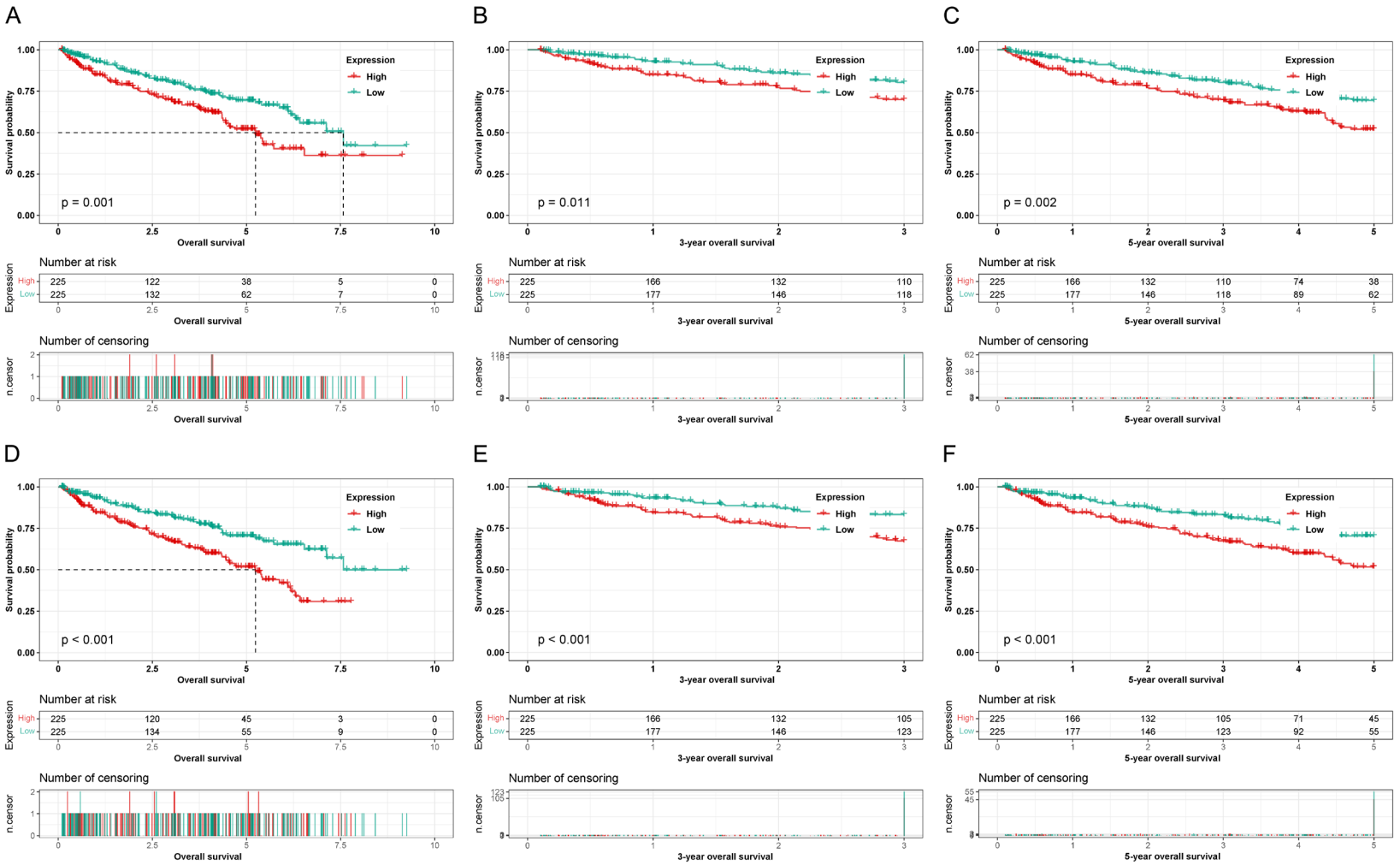

Figure 4. The survival rate of KIRC patient with high expression of 2 CRIncRNAs. A-C. The 1-, 3-, and 5-year survival rate of KIRC patient with high or low LINC01204 expression. D-F. The 1-, 3-, and 5-year survival rate of KIRC patient with high or low LINC01711 expression.

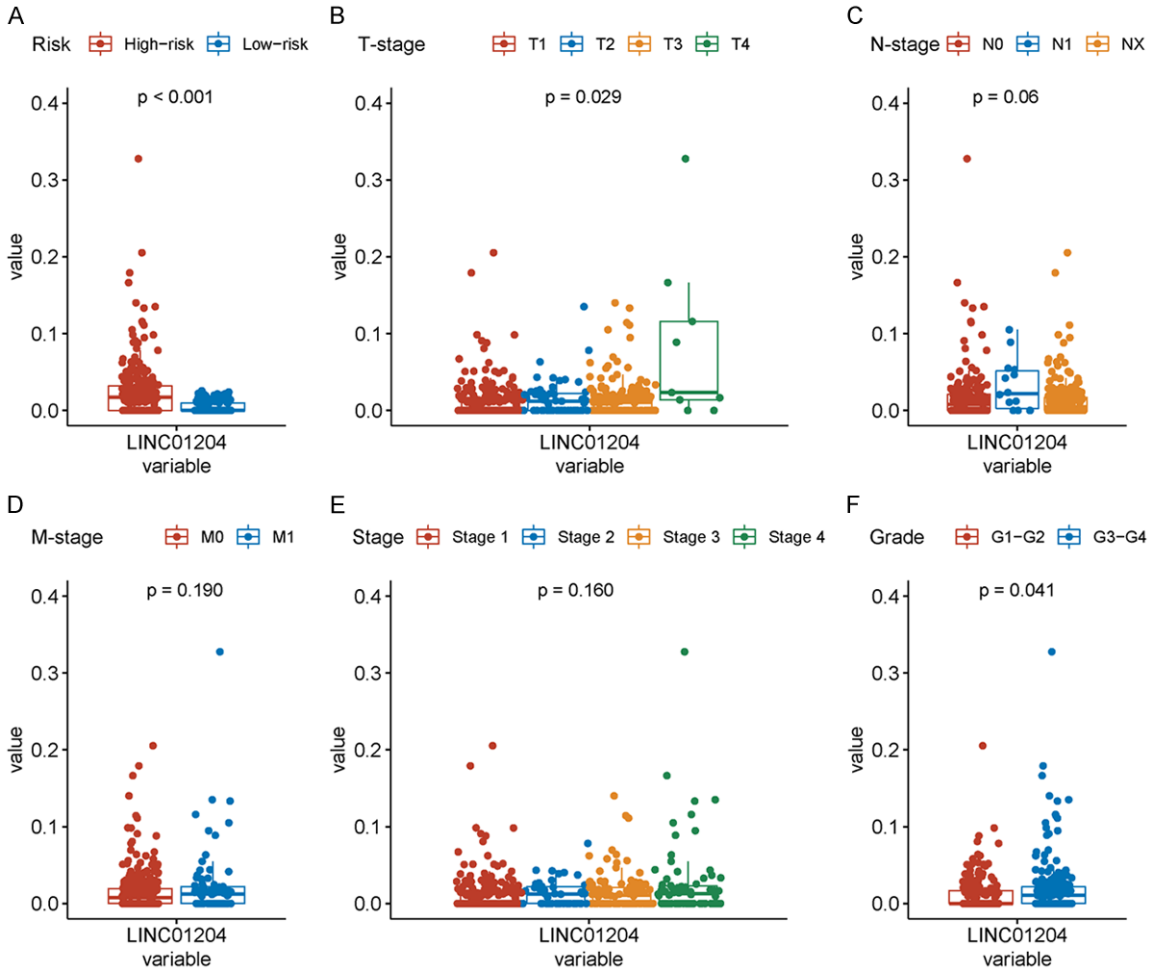

Figure 5. Expression of LINC01204 in KIRC database. (A) Relative expression levels of LINC01204 in high-risk and low-risk groups. (B-F) Difference expression of LINC01204 in TCGA database with T stage (B), N stage (C), M stage (D), pathological stage (E), and tumor grade (F).

3-, and 5-year OS of patients with KIRC (**Figure 3A**). The capability and accuracy of the nomogram were verified by different methods including ROC curves (**Figure 3B**) and calibration curves (**Figure 3C**). As shown in **Figure 3B**, the area under curves for the 1-, 3-, and 5-year OS were 0.84, 0.81, and 0.77, respectively. The calibration curve confirmed the high degree of consistency between the predicted values and the actual values (**Figure 3C**). In addition, univariate and multivariate Cox analysis confirmed LINC01204 and LINC01711 as independent CRlncRNAs for OS (P < 0.05, **Figure 3D**, **3E**).

Validation of LncRNAs in KIRC

To further validate the role of LINC01204 expression in KIRC, Kaplan-Meier survival curve was applied to compare the 1-, 3-, and 5-year OS between the high LINC01204-expression and the low-LINC01204 expression groups (**Figure 4A-C**). Consistent with the risk model, the upregulation of LINC01204 was associated with a worse prognosis, and the *P* value for 1-, 3-, and 5-year OS were 0.001, 0.011, and 0.002, respectively. The similar role of LINC01711 expression was also suggested by Kaplan-Meier curve (**Figure 4D-F**) with significant *P*-values. Furthermore, we found that the expression of LINC01204 was related to the risk model, T stage, and grade (P < 0.05, **Figure 5A**, **5B**, **5F**) but not to N stage, M stage, and pathological stage (P > 0.05, **Figure 5C-E**). However, different from LINC01204, the expression of LINC01711 was associated with the risk model, T stage, M stage, pathological

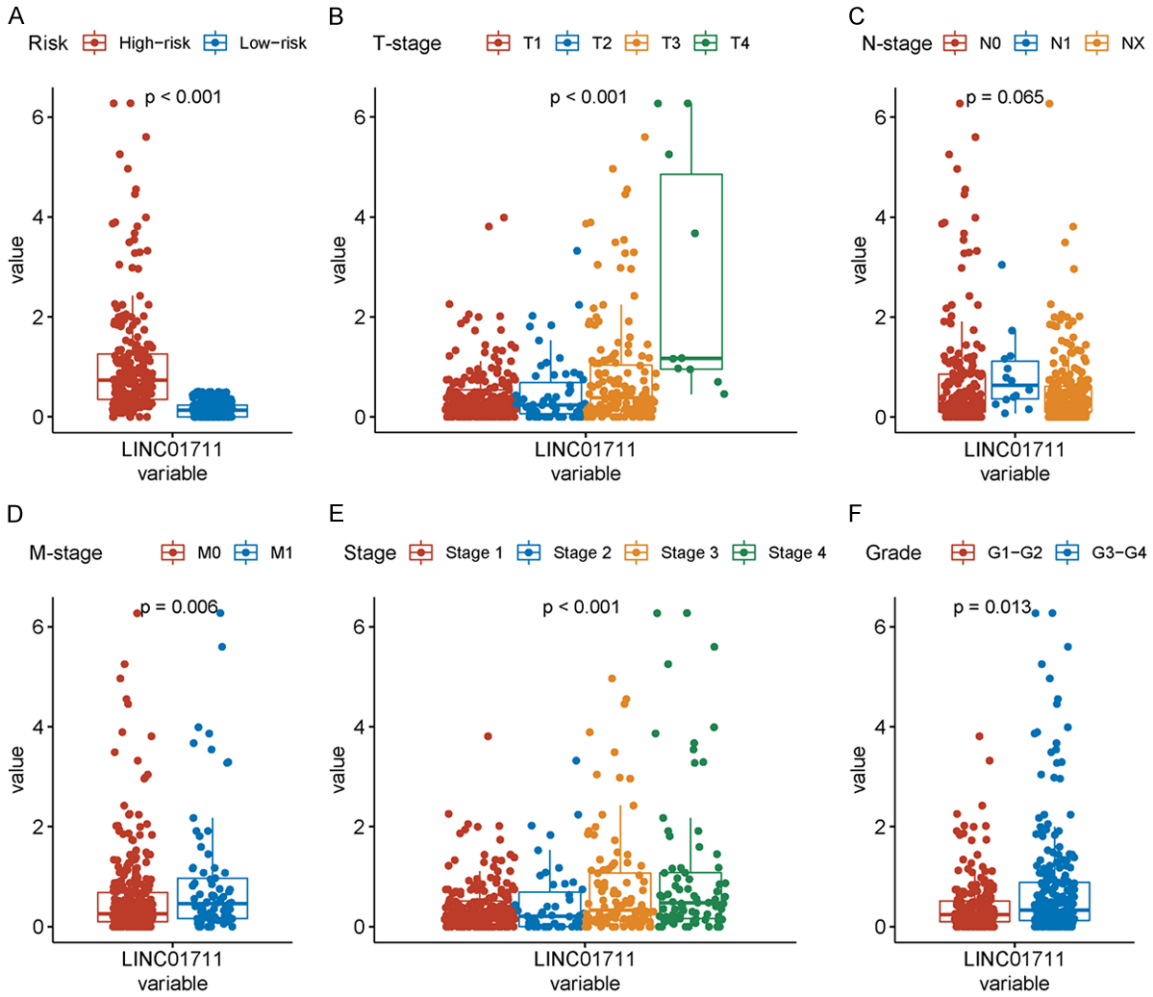

Figure 6. Expression of LINC01711 in KIRC database. (A) Relative expression levels of LINC01711 in high-risk and low-risk groups. (B-F) Difference expression of LINC01711 in TCGA database with T stage (B), N stage (C), M stage (D), pathological stage (E), and tumor grade (F).

stage, and grade ($P < 0.05$, **Figure 6A**, **6B**, **6D-F**) but not with N stage ($P > 0.05$, **Figure 6C**).

Construction of a LncRNA-mRNA co-expression network

The association of mRNA with the two prognostic risk-related CRlncRNAs was analyzed by the Sankey diagram (**Figure 7**), and the results predicted the possible combination of miRNA and mRNA downstream of CRlncRNAs, which shed light on the further mechanistic study of CRlncRNAs.

Knockdown of LINC01711 inhibited the proliferation, migration, and invasion of KIRC cells

Since previous studies have reported that LINC01711 acts as an oncogene in several cancer types [19, 20], we focused our experimental validation on LINC01711. First, we verified the upregulation of LINC01711 in KIRC cells by qRT-PCR assays (**Figure 8A**). Simultaneously, qRT-PCR proved the successful knockdown of LINC01711 by siLINC01711 (**Figure 8A**). In addition, we also assessed the expression of LINC01711 by FISH and confirmed that LINC01711 level was significantly higher in KIRC samples than in the adjacent normal renal tissues (**Figure 8B**). Furthermore, EdU assays revealed that knockdown of LINC01711 significantly inhibited the proliferation of 786-O cells (**Figure 8C**, **8F**), while wound healing assay indicated knockdown of LINC01711 reduced the migration of 786-O cells (**Figure 8D**, **8F**). Consistently, colony formation assay and transwell assays further demonstrated that knockdown of LINC01711 inhibited the proliferation

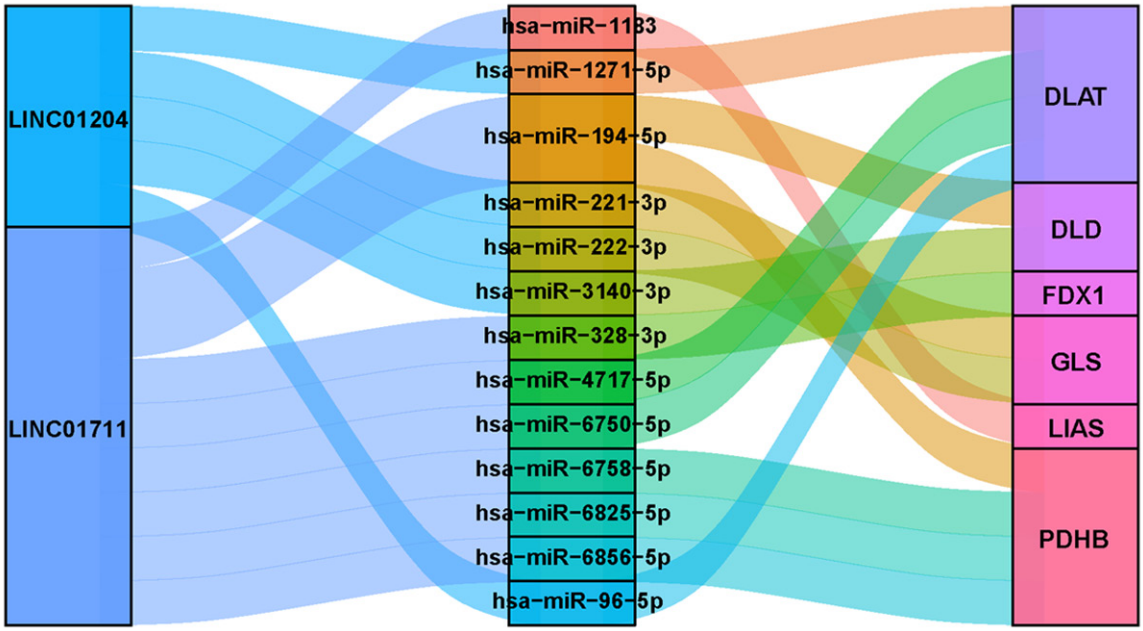

Figure 7. LncRNA-mRNA co-expression network.

and invasion of KIRC cells, respectively (**Figure 8E**, **8F**).

Discussion

In this study, we used lasso regression analysis to identify two prognosis-associated CRlncRNAs (LINC01204 and LINC01711) in KIRC and constructed prognostic risk signatures which were validated in both the training and the validation sets. We further established a prognostic nomogram to predict the 1-, 3-, and 5-year OS. In addition, the Kaplan-Meier survival curve was applied to compare the survival between the high-risk and the low-risk groups. Importantly, both the calibration curves and ROC curves demonstrated the reliability of our model.

Copper, as a catalytic cofactor for essential enzymes, is involved in many cellular processes by regulating oxygen transport, energy conversion and intracellular oxidative metabolism [21]. Hence, it is conceivable that Copper imbalance can disturb the normal metabolism and lead to various diseases [22]. Notable, a growing body of evidence has indicated that copper metabolism is associated with a variety of tumors, and in particular, imbalance in copper homeostasis leads to the development of tumors [23]. Cobine et al. first described copper-dependent cell proliferation which was related to various cellular processes and proposed a new type of cell death termed cuproptosis [24]. Furthermore, Ge et al. reported that copper could also mediate cell death through mitochondria-dependent energy metabolism and reactive oxygen species (ROS) accumulation [25]. Recently, Tsvetkov et al. reported that copper bound to the lipid acylated components of the tricarboxylic acid (TCA) cycle which caused the aggregation of lipid acylated proteins and cell death [26]. The process and regulation of cuproptosis are different from other types of cell death such as apoptosis, necroptosis, as well as ferroptosis and have attracted attentions from different fields of research.

LncRNAs, as a class of RNA molecules, are involved in a variety of physiological and pathological processes including tumorigenesis; nevertheless, there are only few reports on the function of LncRNAs in cuproptosis and the role of CRlncRNAs in KIRC. The study by Li et al. screened 529 glioma samples as well as 5 non-tumor brain tissue samples and found LINC01711 as an independent risk factor [27]. Another study reported that exosomal LINC01711 was differentially expressed in esophageal squamous cell carcinoma (ESCC) and suppressed miR-326 level, whereas it upregulated the expression of fascin actin-bundling protein

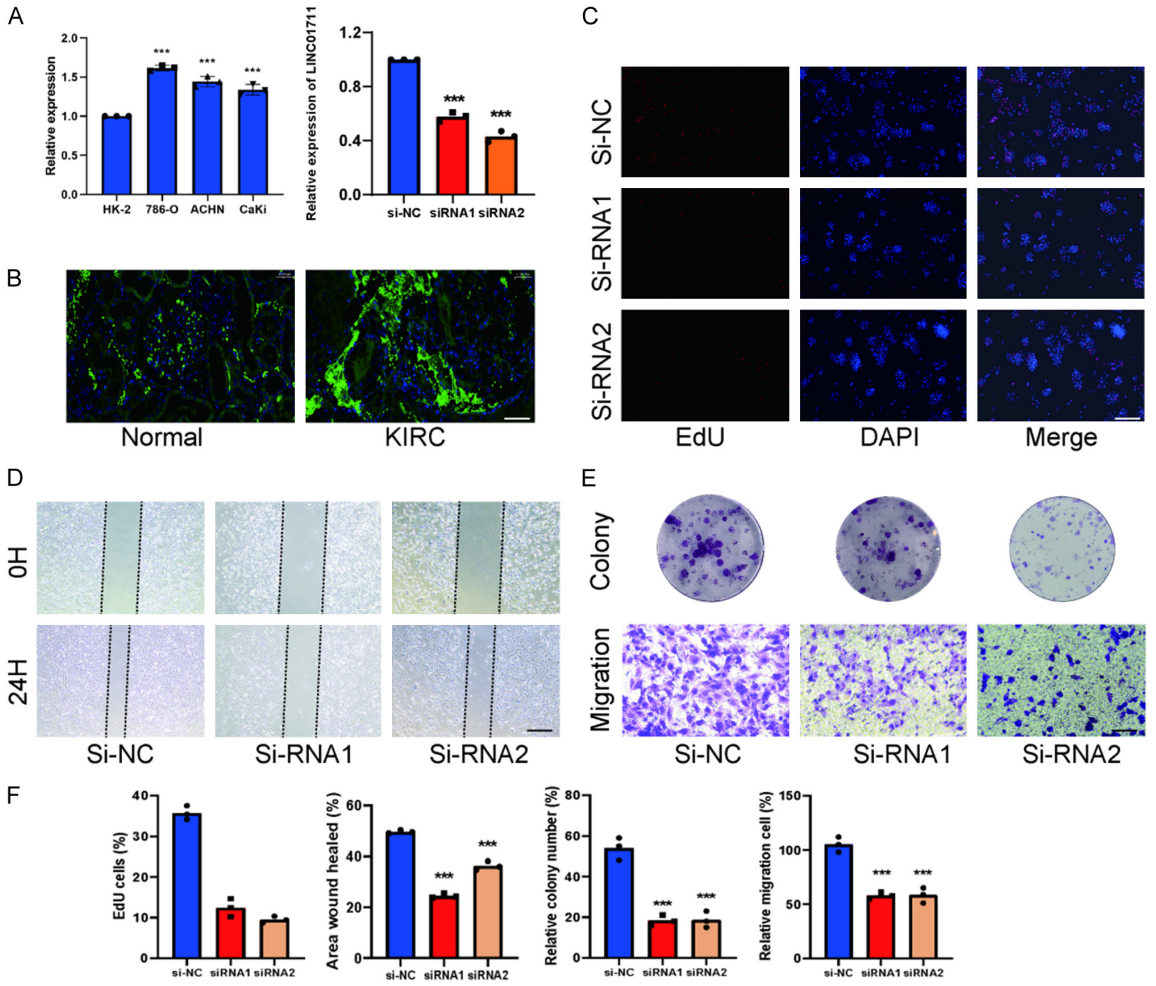

Figure 8. Knockdown of LINC01711 inhibits the proliferation, invasion and migration of KIRC cells. A. qRT-PCR analysis of LINC01711 expression levels in KIRC cell lines. Expression of LINC01711 was confirmed by qRT-PCR in KIRC cell lines transfected with si-NC, si-RNAs in 786-O cells. B. Expression levels of LINC01711 was detected by RNA FISH in tumor samples and compared tissues in human samples. FAM-labeled probes for detecting LINC01711 were synthesized by Genepharma (Genepharma Biotechnology, Shanghai, China). C. EdU assay of cell proliferation capacity of 786-O cells after transfection with si-NC, si-RNA1 and si-RNA2. D. Wound healing assay of cell migration capacity of 786-O cells after transfection with si-NC, si-RNA1 and si-RNA2. E. Transwell assay results for cell invasion and colony experiments in 786-O cells after transfection with si-NC, si-RNA1 and si-RNA2. F. The statistical results of the above functional experiments. *P < 0.05, **P < 0.01, ***P < 0.001, Scale bar: 100 um.

1 to promote the occurrence and development of ESCC [20]. However, the role of LINC01711 in KIRC was still unknown. In this study, we investigated the function of LINC01711 and determined its oncogenic role in KIRC. Therefore, our study provided evidence for using LINC01711 as a potential biomarker for the early diagnosis and prognosis of patients with KIRC.

In conclusion, we identified two CRlncRNAs using the TCGA-KIRC dataset and constructed prognostic risk signatures. In addition, we showed that the prognostic nomograms could accurately predict the OS of KIRC patients. Finally, we experimentally validated the function of LINC01711 in the proliferation, migration, and invasion of KIRC cells.

Acknowledgements

The authors thank all the patients who trusted them and all the physicians and staff who helped them in this study. This work was supported by National Natural Science Foundation of China (Grant No. 82270809).

Disclosure of conflict of interest

None.

Address correspondence to: Weipu Mao, Department of Urology, Shanghai Putuo District People's Hospital, School of Medicine, Tongji University, Shanghai 200060, China. Tel: +86-18621571327; Fax: +86-18621571327; E-mail: maoweipu88@163.com

References

[1] Sung H, Ferlay J, Siegel RL, Laversanne M, Soerjomataram I, Jemal A and Bray F. Global cancer statistics 2020: GLOBOCAN estimates of incidence and mortality worldwide for 36 cancers in 185 countries. CA Cancer J Clin 2021; 71: 209-249.

[2] Leibovich BC, Lohse CM, Crispen PL, Boorjian SA, Thompson RH, Blute ML and Cheville JC. Histological subtype is an independent predictor of outcome for patients with renal cell carcinoma. J Urol 2010; 183: 1309-1315.

[3] Batavia AA, Schraml P and Moch H. Clear cell renal cell carcinoma with wild-type von Hippel-Lindau gene: a non-existent or new tumour entity? Histopathology 2019; 74: 60-67.

[4] Maxwell PH, Wiesener MS, Chang GW, Clifford SC, Vaux EC, Cockman ME, Wykoff CC, Pugh CW, Maher ER and Ratcliffe PJ. The tumour suppressor protein VHL targets hypoxia-inducible factors for oxygen-dependent proteolysis. Nature 1999; 399: 271-275.

[5] Kahlson MA and Dixon SJ. Copper-induced cell death. Science 2022; 375: 1231-1232.

[6] Ding X, Jiang M, Jing H, Sheng W, Wang X, Han J and Wang L. Analysis of serum levels of 15 trace elements in breast cancer patients in Shandong, China. Environ Sci Pollut Res Int 2015; 22: 7930-7935.

[7] Baltaci AK, Dundar TK, Aksoy F and Mogulkoc R. Changes in the serum levels of trace elements before and after the operation in thyroid cancer patients. Biol Trace Elem Res 2017; 175: 57-64.

[8] Zhang X and Yang Q. Association between serum copper levels and lung cancer risk: a meta-analysis. J Int Med Res 2018; 46: 4863-4873.

[9] Saleh SAK, Adly HM, Abdelkhaliq AA and Nassir AM. Serum levels of selenium, zinc, copper, manganese, and iron in prostate cancer patients. Curr Urol 2020; 14: 44-49.

[10] Basu S, Singh MK, Singh TB, Bhartiya SK, Singh SP and Shukla VK. Heavy and trace metals in carcinoma of the gallbladder. World J Surg 2013; 37: 2641-2646.

[11] Shanbhag VC, Gudekar N, Jasmer K, Papageorgiou C, Singh K and Petris MJ. Copper metabolism as a unique vulnerability in cancer. Biochim Biophys Acta Mol Cell Res 2021; 1868: 118893.

[12] Lelievre P, Sancey L, Coll JL, Deniaud A and Busser B. The multifaceted roles of copper in cancer: a trace metal element with dysregulated metabolism, but also a target or a bullet for therapy. Cancers (Basel) 2020; 12: 3594.

[13] Li Y. Copper homeostasis: emerging target for cancer treatment. IUBMB Life 2020; 72: 1900-1908.

[14] Tsvetkov P, Coy S, Petrova B, Dreishpoon M, Verma A, Abdusamad M, Rossen J, Joesch-Cohen L, Humeidi R, Spangler RD, Eaton JK, Frenkel E, Kocak M, Corsello SM, Lutsenko S, Kanarek N, Santagata S and Golub TR. Copper induces cell death by targeting lipoylated TCA cycle proteins. Science 2022; 375: 1254-1261.

[15] Ouyang J, Zhong Y, Zhang Y, Yang L, Wu P, Hou X, Xiong F, Li X, Zhang S, Gong Z, He Y, Tang Y, Zhang W, Xiang B, Zhou M, Ma J, Li Y, Li G, Zeng Z, Guo C and Xiong W. Long non-coding RNAs are involved in alternative splicing and promote cancer progression. Br J Cancer 2022; 126: 1113-1124.

[16] Mercer TR, Dinger ME and Mattick JS. Long non-coding RNAs: insights into functions. Nat Rev Genet 2009; 10: 155-159.

[17] Muller V, Oliveira-Ferrer L, Steinbach B, Pantel K and Schwarzenbach H. Interplay of lncRNA H19/miR-675 and lncRNA NEAT1/miR-204 in breast cancer. Mol Oncol 2019; 13: 1137-1149.

[18] Wang K, Gu Y, Ni J, Zhang H, Wang Y, Zhang Y, Sun X, Xu T, Mao W and Peng B. Noncoding-RNA mediated high expression of zinc finger protein 268 suppresses clear cell renal cell carcinoma progression by promoting apoptosis and regulating immune cell infiltration. Bioengineered 2022; 13: 10467-10481.

[19] Shi X, Liu X, Pan S, Ke Y, Li Y, Guo W, Wang Y, Ruan Q, Zhang X and Ma H. A novel autophagy-related long non-coding RNA signature to predict prognosis and therapeutic response in esophageal squamous cell carcinoma. Int J Gen Med 2021; 14: 8325-8339.

[20] Xu ML, Liu TC, Dong FX, Meng LX, Ling AX and Liu S. Exosomal lncRNA LINC01711 facilitates metastasis of esophageal squamous cell carcinoma via the miR-326/FSCN1 axis. Aging (Albany NY) 2021; 13: 19776-19788.

[21] Kim BE, Nevitt T and Thiele DJ. Mechanisms for copper acquisition, distribution and regulation. Nat Chem Biol 2008; 4: 176-185.

[22] Lutsenko S. Human copper homeostasis: a network of interconnected pathways. Curr Opin Chem Biol 2010; 14: 211-217.
[23] Shanbhag VC, Gudekar N, Jasmer K, Papageorgiou C, Singh K and Petris MJ. Copper metabolism as a unique vulnerability in cancer. Biochim Biophys Acta Mol Cell Res 2021; 1868: 118893.
[24] Cobine PA, Moore SA and Leary SC. Getting out what you put in: copper in mitochondria and its impacts on human disease. Biochim Biophys Acta Mol Cell Res 2021; 1868: 118867.
[25] Ge EJ, Bush AI, Casini A, Cobine PA, Cross JR, DeNicola GM, Dou QP, Franz KJ, Gohil VM, Gupta S, Kaler SG, Lutsenko S, Mittal V, Petris MJ, Polishchuk R, Ralle M, Schilsky ML, Tonks NK, Vahdat LT, Van Aelst L, Xi D, Yuan P, Brady DC and Chang CJ. Connecting copper and cancer: from transition metal signalling to metalloplasia. Nat Rev Cancer 2022; 22: 102-113.
[26] Tsvetkov P, Coy S, Petrova B, Dreishpoon M, Verma A, Abdusamad M, Rossen J, Joesch-Cohen L, Humeidi R, Spangler RD, Eaton JK, Frenkel E, Kocak M, Corsello SM, Lutsenko S, Kanarek N, Santagata S and Golub TR. Copper induces cell death by targeting lipoylated TCA cycle proteins. Science 2022; 375: 1254-1261.
[27] Li X and Meng Y. Survival analysis of immune-related lncRNA in low-grade glioma. BMC Cancer 2019; 19: 813.